ISSN: 0067-2904

Investigation of Shielding for Fast Neutrons Using Polymer Composites with Pb Reinforcement

Fadhel Mahmood Hmood[1,2]*, Hayder S. Hussain[1]
[1]*Physics Department, College of Science, Baghdad University, Baghdad, Iraq*
[2]*National Monitoring Authority, Ministry of Science and Technology, Baghdad, Iraq*

Received: 5/6/2022 Accepted: 1/3/2023 Published: 30/12/2023

Abstract

Manufacturing high-efficiency polymeric materials to moderate fast neutrons by converting them into slow or thermal neutrons. These materials absorb thermal neutrons as well as gamma rays associated with neutrons. Materials of small mass number are used to slow down fast neutrons because neutrons have a high cross-section when they interact with these materials. Materials of high mass number absorb gamma rays. Polyurethane and epoxy were mixed in various ratios to create a blend to serve as neutrons shield, lead (Pb) was then added to the blend at weight percentages of 20%, 30%, 40%, 50%, and 70% to produce a polymer composite.

Polymeric materials reinforced with lead in various ratios were tested to select the best composite. The Polymeric samples were placed between the neutron source and the detector, and changing their thickness from 1 cm to 10 cm in increments of 1 cm. The neutron count rate for five readings was recorded, and the average was taken. As a result, the relationship between count rate and sample thickness was plotted, the half-value thickness of the shield was determined, the relationship between the logarithm (I_0/I) and the thickness was drawn, the removal cross-section ($\sum_R$) was determined, as well as, the mean free path of the fast neutron, and these were compared for each sample. This work concluded that the sample containing 20% lead with a thickness of 10 cm and a diameter of 4 cm was the best shielding for absorbing fast neutrons.

Keywords: polymer composite; fast Neutron; removal cross section; count rate; half-value thickness.

فحص أداء تدريع النيوترونات السريعة بواسطة متراكبات بوليمرية مدعمة بالرصاص

فاضل محمود حمود[1,2]*، حيدر سليم حسين[1]
[1]قسم الفيزياء، كلية العلوم، جامعة بغداد، بغداد، العراق
[2]هيئة الرقابة الوطنية، وزارة العلوم والتكنولوجيا، بغداد، العراق

الخلاصة

تم تصنيع مواد بوليمرية ذات كفاءة عالية لتهدئة النيوترونات السريعة بواسطة تحويل النيوترونات السريعة إلى نيوترونات بطيئة أو حرارية، ومن ثم امتصاص النيوترونات الحرارية وكذلك امتصاص أشعة كاما المرافقة للنيوترونات. ان استخدام مواد ذات عدد كتلي صغير تعمل على ابطاء النيوترونات السريعة، وذلك لكون

* Email: fmh_1968@yahoo.com

النيوترون يمتلك مقطع عرضي عالي عند تفاعله مع المواد ذات العدد الكتلي الصغير، اما المواد ذات العدد الكتلي العالي فتمتص أشعة كاما. تم خلط الايبوكسي مع البولي يوريثان بنسب مختلفة للحصول على مزيج البوليمر. بعد ذلك تم اضافة مسحوق الرصاص بنسب وزن 20٪، 30٪، 40٪، 50٪، 70٪ لتكوين المتراكب البوليمري. تم اختبار المواد البوليمرية المدعمة بالرصاص بنسب مختلفة من أجل اختيار أفضل مركب، حيث تم وضع العينات بين المصدر النيوتروني والكاشف، وبدءًا من 1 سم إلى 10 سم بزيادة قدرها 1 سم، تم تسجيل خمس قراءات لمعدل العد للنيوترونات ثم أخذ المعدل. تم رسم العلاقة بين معدل العد وسمك العينة، وتم تحديد قيمة نصف السمك للدرع، ثم تم رسم العلاقة بين لوغاريتم (I_0/I) وسمك العينة، تم تحديد المقطع العرضي للإزالة ($\sum_R$) ومن ثم حساب متوسط المسار الحر للنيوترون، ومقارنة النتائج لكل عينة. خلال هذا البحث وجد بأن العينة المتكونة من 20% رصاص بسمك 10سم وقطر4 سم هي أفضل درع لامتصاص النيوترونات السريعة.

1 Introduction

Radiation shielding entails putting a shielding material between the source of ionizing radiation and the worker or the environment. The radiations that must be addressed are X and gamma rays, alpha particles, beta particles, and neutrons. Each kind of radiation interacts with shielding material in a different way. As a result, the efficiency of shielding varies with the kind and energy of radiation, as well as with the shielding material utilized [1].

Neutron particles are neutral, and since they do not carry a charge capable of penetrating nuclei, their interaction with matter varies from that of photons. The primary response mechanisms with nuclei are elastic and inelastic scattering and absorption [2].

In elastic scattering interactions, the neutron interacts with the nucleus, which is generally stable and subject to momentum and energy conservation principles, on the other hand, the inelastic scattering interactions, leave the nucleus in an excited state following the reaction and are followed by the return of the excited nucleus to the ground stable state through gamma ray emission. In terms of absorption reactions, the neutron is absorbed and retained by the nucleus, converting it into an unstable radioactive nucleus, and the nucleus removes the excess energy to return to stability by releasing gamma rays [3].

Neutron shielding is complicated because neutrons interact with matter exclusively through nuclei, which means they do not readily stop through matter and may travel long distances without scattering or absorption. This indicates that neutrons have a high penetrability ability, making them hazardous in material and radiation considerations. The removal cross-section, mean free path, and half-value thickness, are used to characterize neutron interactions with materials [4].

Composites can be used for shielding. A composite material is made up of two or more materials. They are defined by their capacity to combine the properties of their constituent materials while overcoming each material shortcomings individually. Polymeric-based composite materials were utilized in this work. It is resistant to corrosion and rust and can be shaped into various shapes and sizes due to its light weight and ability to withstand chemicals. Specific neutron absorbent and conductive elements were incorporated into the composite structure to create a new design for shielding materials [5,6].

2 Experimental and calculation methods

2.1 Materials and sample preparation

The shielding material used was a combination of two materials (called a blend) of different concentrations, which are epoxy (EUXIT 50 KII) and polyurethane (Euxit TG-10) (made in Egypt by the Egyptian Swiss for Industry and Trading Co.). The blend was reinforced with lead powder (Pb) of different weight ratios. The lead percentages were (20, 30, 40, 50, 70) wt.% for samples A, B, C, D, and E, respectively, which were mixed using blend ratios and produced polymer composites that were calculated to be 100 per cent weight in total. Each sample is 1cm thick and 4 cm in diameter, as shown in Figure 1. For the attenuation measurements for each composite, its thickness was changed in the range (1-10) cm increments of 1cm.

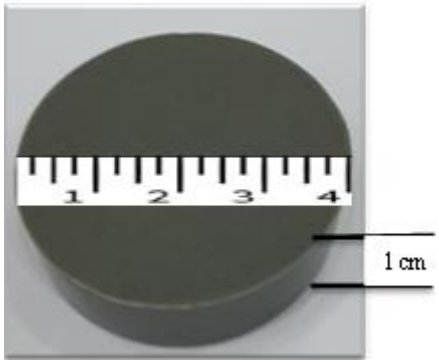

Figure 1: Composite sample.

2.2. Preparation of the collimator

^{241}Am-Be was the neutron source used. A collimator was made up of different components to get a neutron beam. A narrow tube with a diameter of 4 cm and a height of 10 cm was placed in the center of a larger tube of the same height with a diameter of 11.5 cm. A polymer substance was poured in the vacancy between the two tubes. The collimator's overall length was 10 cm, as shown in Figure 2. The distance between the source and the detector was fixed at 30 cm by utilizing a 20-cm-long permanent collimator, which was made of paraffin wax.

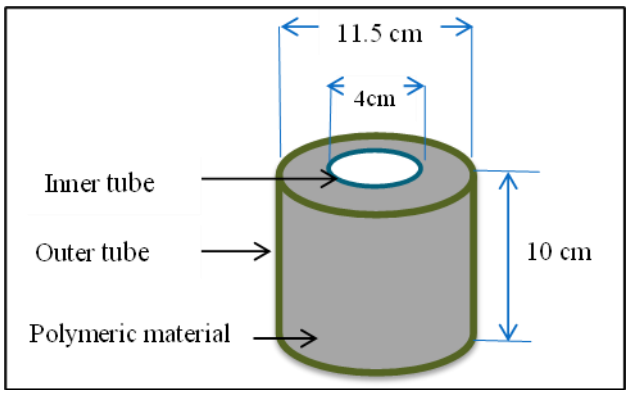

Figure 2: Polymeric collimator

2.3. Experiment work

Figure 3 shows the experimental setup; the center of the detector and the center of the neutron beam are in a straight line. The neutron detector was placed at a fixed distance of 30 cm from the ^{241}Am-Be neutron source. This distance was chosen after conducting tests to determine if the neutron detector should be oriented perpendicular to the direction of the output neutron beam, which records the directly transmitted neutrons. Five values of neutron count rate were recorded, and the average rate was calculated; the count rate was measured to be 38.4

n/s at x=0; this represents the initial value I_0. Shielding samples were made of polymer composite reinforced by 20%, 30%, 40%, 50%, and 70% weight of lead with dimensions of 1cm thick and 4 cm diameter. Different thicknesses of the shielding sample for every concentration were tested.

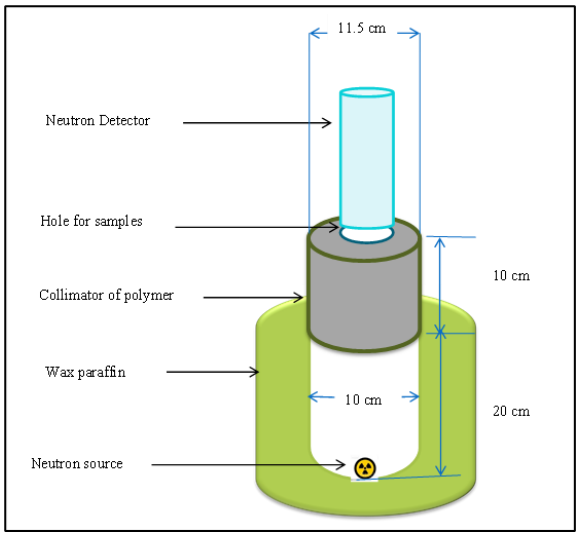

Figure 3: Experimental setup

2.4. Neutron measurements

The measurements were carried out using a collimated neutron beam from the $^{241}_{95}Am$–Be source. The neutron beam was tested using different samples, the neutrons count rate (n/s) from the neutron source was measured with no sample between the source and the detector, the neutron count rate was measured again with a different thickness of the sample (1cm-10 cm) placed between the source and the detector.

The neutron count rate was measured with a neutron detector type Inspector 1000 (manufactured by Canberra Industries, Inc. USA), neutron probe-external detector; moderated $^{3}_{2}He$ tube (8 cm active length, 2atm); intrinsic neutron sensitivity ≈1%, using an unmoderated $^{252}_{98}Cf$ fast neutron source, mass equal to 1.36 kg [7].

2.5. Basic knowledge

2.5.1. Neutron attenuation

When neutron attenuated, the effective removal cross-section $\sum_R$ of a particular material behaves formally as a macroscopic cross-section determined by drawing the relationship between the count rate and the thickness. Because all interactions tend to remove energy from the fast neutron beam, the $\sum_R$ value is not different to the total (scattering and capture) macroscopic cross-section $\sum_t$ of the material. Neutron shielding is complicated due to the fact that neutrons are not easily attenuated by matter since they interact with atoms of matter solely through their nuclei. As a result, the shield material's combined removal coefficient $\sum_R$ (cm^{-1}) was calculated experimentally. The exponential absorption equation is used to get reasonable conclusions concerning the attenuation of fast neutrons utilizing these effective removal cross-sections [8,9].

$$I = I_0 e^{-\sum_R X} \quad (1)$$

where I_0 represents the initial neutron count rate for a shield thickness of 0 cm, and I represent the count rate for a shield thickness of X cm. In general, the attenuation of neutrons as they travel through a medium is determined by the microscopic cross-section (σ), which

follows the $1/v$ law (v is the velocity of neutron), and the number of atoms or molecules per unit volume N_0 (atom density) within the medium. Total macroscopic cross-section $\sum_t$, a physical quantity that connects these two elements, can be determined by [10,11].

$$\sum_t = N_0\sigma \quad (2)$$

N_0 is given by where $N_0 = \frac{\rho}{M}N_A$ where N_A is the Avogadro's number, M is molecular weight of the material. For energies between 2 and 12 MeV, the effective removal cross-section will be almost constant and when the traversed medium contains a large amount of hydrogen, it will be $\sum_R = \sum_t$ and when materials contain a small fraction of hydrogen $\sum_R = \frac{2}{3}\sum_t$ for energy between 6-8 MeV [12].

The effective removal cross-section for compounds and homogeneous mix may be estimated using the values $\sum_R(cm^{-1})$ or $\sum_R/\rho(cm^2.g^{-1})$, for various elements in the compounds or mixtures, as shown in Eq. (3), where w_i is the partial density ($g.cm^{-3}$) and corresponds to *ith* constituent density. Then [13,14]:

$$\sum_R = \sum w_i \ (\sum_R/\rho)_i \quad (3)$$

2.5.2. Half-value layer (HVL)

The half-value thickness (cm) is a useful radiation shielding metric that displays half-thickness ($X_{1/2}$) exponential attenuation of the neutrons. It is the thickness of absorber necessary to reduce the intensity of a beam to one-half its initial value. The HVL is defined as the thickness of material necessary to reduce the starting value of counts by half. The following equation can be used to compute it: [15,16].

$$\frac{I}{I_0} = \frac{1}{2} = e^{-\sum_R X_{1/2}} \quad (4)$$

2.5.3. Mean free path (MFP)

The average distance between two subsequent contacts, or the average distance that a neutron may gain in the material without interacting, is expressed as the mean free path (λ) with length dimensions. The interaction probability of the neutron is extremely low at this distance. A link exists between a neutron's mean free path and its removal cross-section, which may be proven as follows [17].

$$\lambda(cm) = \frac{\int_0^\infty xe^{-\Sigma x}dx}{\int_0^\infty e^{-\Sigma x}dx} = \frac{1}{\sum_R} \quad (5)$$

3. Results and discussion

The neutron count rate for each sample, placed in front of the detector, of different thicknesses in the range (1-10) cm increments of 1cm was recorded.

Displaying the relation between neutron count rate (I) and sample thickness (X) of each Pb concentration, the thickness value required to bring the count rate value down to half its maximum value was determined. Through the relationship between the logarithm (I_0/I) and the sample thickness of each concentration (eq. 4), the value of the neutron removal cross-section was found, and the mean free path was determined.

Figure 4a represents the relationship between the neutron count rate and the thickness of composite sample (A), that consists of 20% Pb and 80% blend.

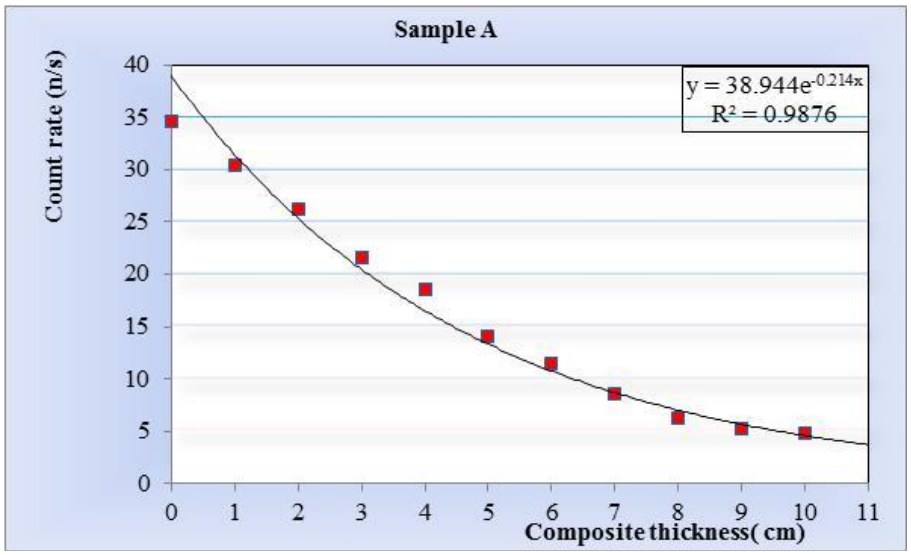

Figure 4 a: Neutron count rate versus composite (of 20% Pb) thickness.

From this figure, it can be noted that the count rate decreased as the thickness of the composite samples in front of the detector increased because of the absorption of the thermal neutrons. From the graph, the HVL can be determined to be equal to 3.1cm. 1 cm composite thickness decreased the count rate of neutrons by 12%, while a thickness of 10 cm decreased the neutrons count rate by 86%, with respect to the initial value.

Figure 4b represents the relationship between ln (I_0/I) and the sample thickness. It is clear that ln (I_0/I) increases with the thickness increase. From this graph, $\sum_R$ of fast neutron and λ can be calculated, equal to 0.215$cm^{-1}$and 4.651cm, respectively.

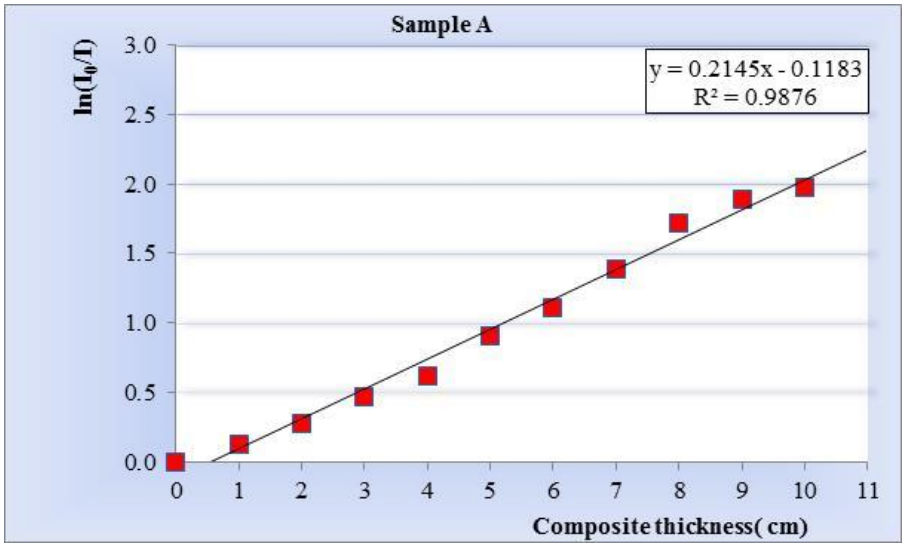

Figure 4b: The variation of ln (I_0/I) with composite (of 20% Pb) thickness.

Figure 5a shows the relationship between the neutron count rate and the composite sample (B) thickness formed of 30% lead and 70% polymeric material.

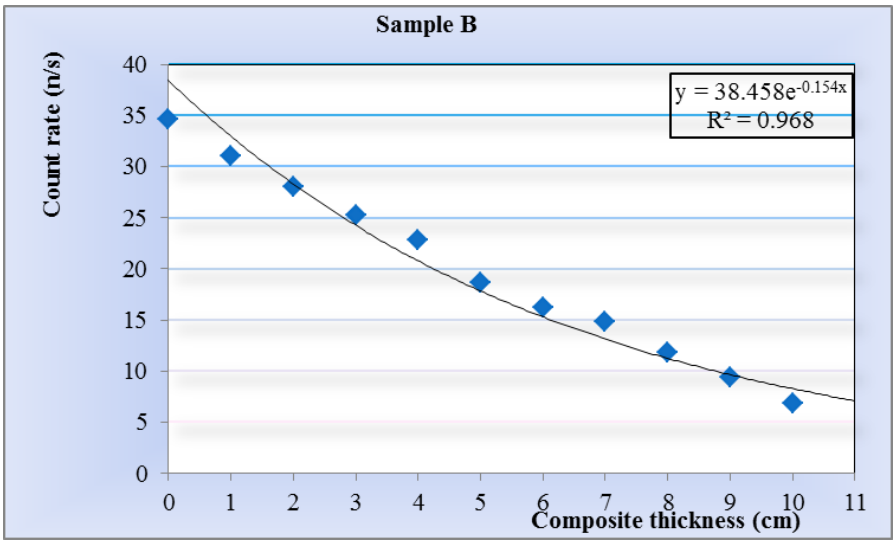

Figure 5a: Neutron count rate versus composite (of 30% Pb) thickness.

From Figure 5a, the graph shows that the value of the count rate falls as the thickness of the composite increases, allowing one to determine the half-value thickness of the composite. The value of X needed to get the neutron count rate down to 19.2 n/s is 4.2cm, the value of the neutron count rate decreased by 10% of its initial value when using 1cm of the composite, while it decreased by 80% of the initial value when using a thickness of 10 cm.

Figure 5b displays the relation between ln (I_0/I) and the sample thickness.

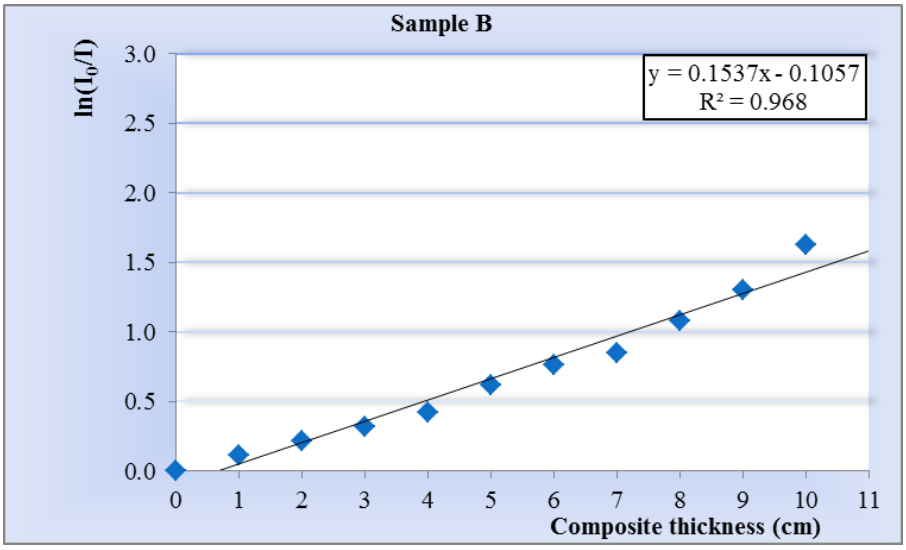

Figure 5b: The variations of ln(I_0/I) versus composite (of 30% Pb) thickness.

The figure shows that the value of ln(I_0/I) increases with the rise in composite thickness. From the graph, one can calculate $\sum_R$, which was equal to $0.154cm^{-1}$, λ was also evaluated to be equal to 6.494cm. Concerning the mean free path values, it was found that there was a 39% rise in the values of λ when utilizing sample B of 30% lead as compared to sample A of 20% lead.

Figure 6a shows the relationship between the neutron count rate (I) and the thickness of the composite sample (C), composed of 40% lead and 60% polymer blend.

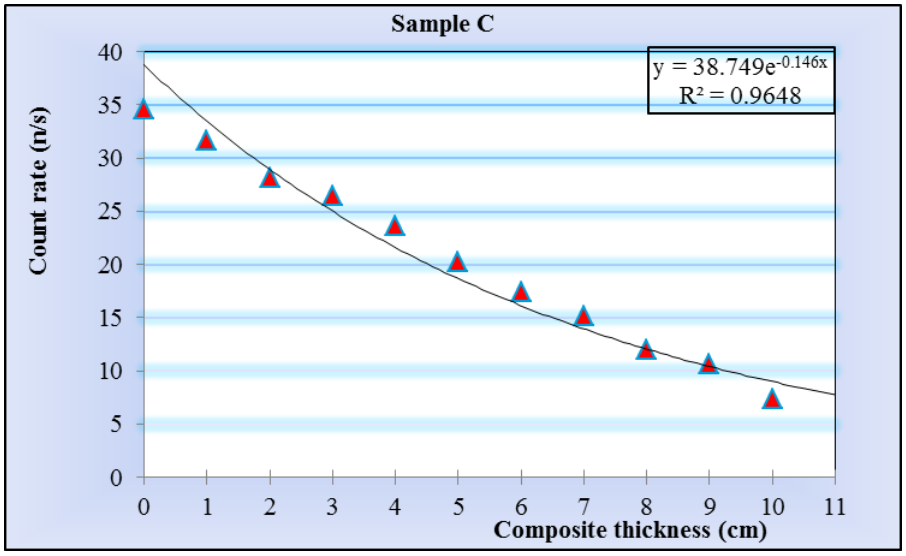

Figure 6a: Neutron count rate versus composite (of 40% Pb) thickness.

The diagram shows a clear decrease in neutron count rate as the thickness of the composite sample increases. From the exponential relation and the intersection of the neutron count rate with the thickness, one can find the value of $X_{1/2}$ which was 4.6 cm. The neutron count rate decreased by 8% with 1cm composite thickness, while it decreased by 78% of its initial value with a thickness of 10 cm.

To find out the value of the removal cross-section of neutron, as well as to find out the value of λ, a graphic relationship was drawn between $\ln(I_0/I)$ and the composite thickness, as illustrated in Figure 6b, where the value of $\sum_R$ in this case was $0.146 cm^{-1}$ and the value of the mean free path was 6.849 cm.

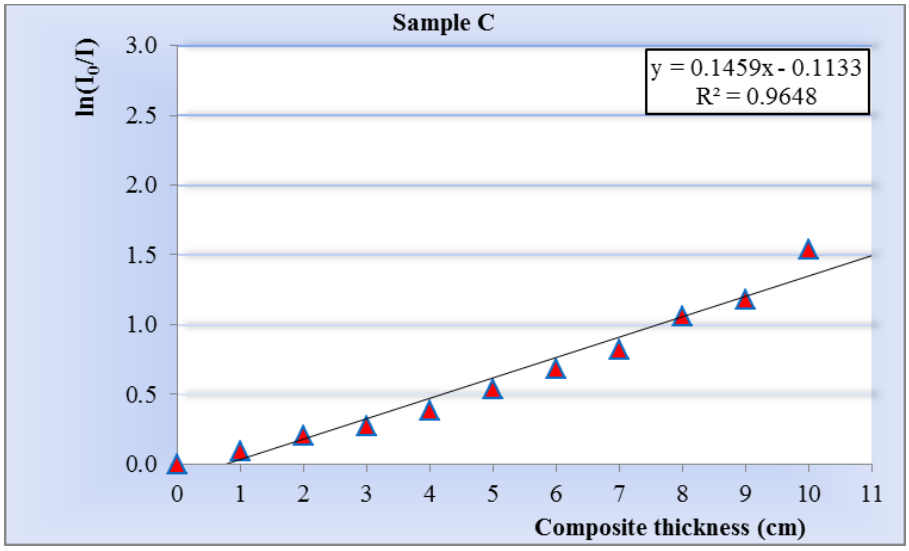

Figure 6b: The variation of $\ln(I_0/I)$ with composite (of 40% Pb) thickness.

Figure 7a shows the relationship between (I) and the composite sample (D) thickness, that consists of 50% Pb and 50% polymer blend.

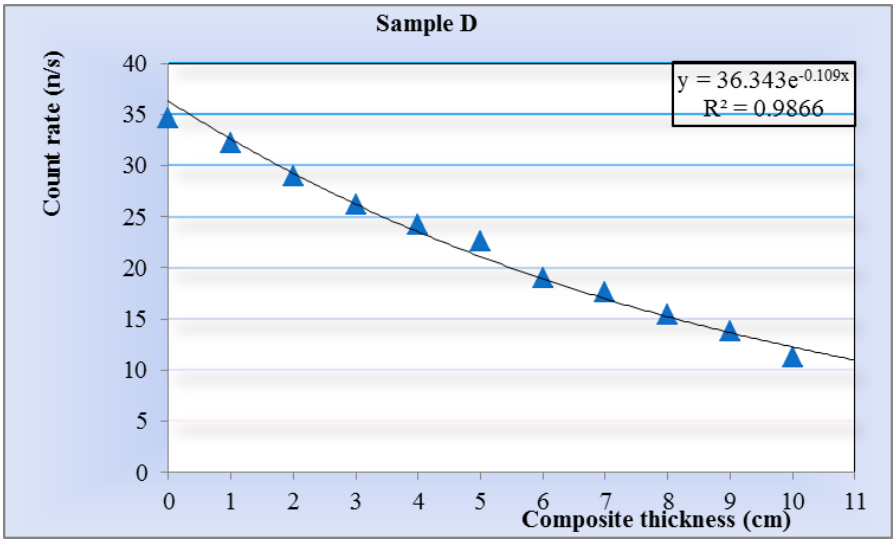

Figure 7a: Neutron count rate versus composite (of 50% Pb) thickness.

From the figure it is observed that the count rate decreased with increasing the composite thickness, the value of $X_{1/2}$ was found to be equal to 6.2 cm. From the obtained values, it was found that the count rate value when placing 1cm of the polymeric material decreased by a very small percentage compared to the initial value, the percentage decrease was only 7%; in the same context, placing a 10 cm thickness of the substance in front of the detector, the percentage count rate was reduced by 67%.

Figure 7b shows the relation between $\ln(I_0/I)$ and the composite thickness.

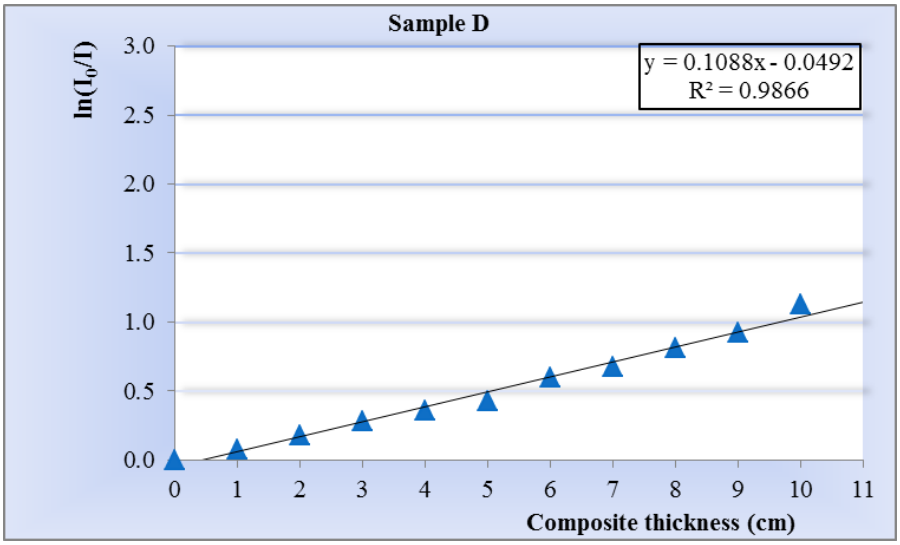

Figure 7b: The variation of $\ln(I_0/I)$ with the composite (of 50% Pb) thickness.

From the figure, the relationship shows that $\ln(I_0/I)$increased as the thickness of the composite increased. The removal cross section of neutrons and the mean free path were $0.109 cm^{-1}$ and 9.174 *cm*, respectively.

Figure 8a depicts the connection between the neutron count rate and the composite sample (E) thickness which was made up of 70% Pb and 30% polymer blend.

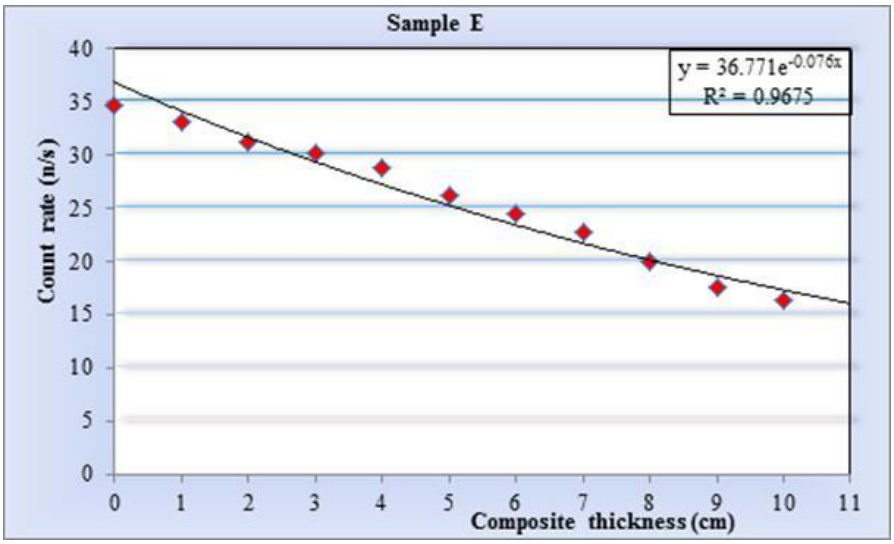

Figure 8a: Neutron count rate versus composite (of 70% Pb) thickness.

From the figure, the graph shows that the count rate falls as the composite thickness increases. The value of $X_{1/2}$was determined to be 9.0 cm. The percentage of neutron count rate decreased by 4%, which is a very small percentage, when placing 1cm of the polymer, while the percentage decrease of the count rate was 52% with 10 cm substance thickness, which is a small percentage when compared to the samples of low concentrations of lead.

Figure 8b shows the relation between $\ln(I_0/I)$ and composite sample (E) thickness.

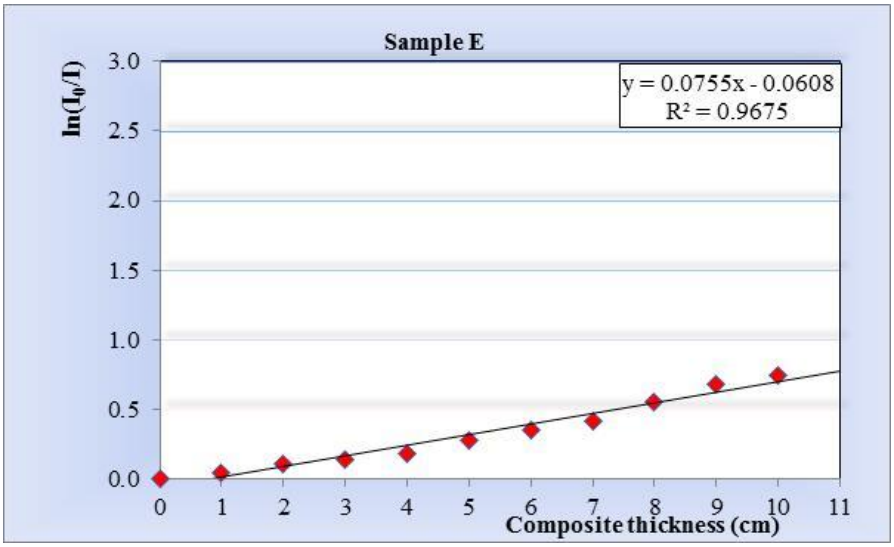

Figure 8b: The variations of $\ln(I_0/I)$ with the composite (of 70% Pb) thickness.

The graph indicates that as the thickness of the composite increases, $\ln(I_0/I)$ increase. The removal cross section of neutrons and the mean free path was calculated to be 0.076 cm^{-1} and 13.158 cm, respectively.

The removal cross-section value decreases as the concentration of lead increases in the composite. The composite with a concentration of 20% lead is preferred over the other prepared concentrations when comparing the values of $X_{1/2}$, while it was found that by increasing the

percentage of lead in the composite, a greater thickness is required to reduce the count rate value by half.

As for comparing the mean free path values, the best value was when using samples with a concentration of 20% lead, the obtained results show that the mean free path value increased with increasing lead concentration.

4. Conclusions

Sample (A), consisting of 20% Pb and 80% blend, has the most efficient characteristics as a shielding material against ^{241}Am-^{9}Be neutrons source. The half-value thickness was 3.1 cm, a removal cross-section of $0.215 cm^{-1}$, and a mean free path of 4.651 cm. Therefore, it is clear that the best concentration that can be used as an effective neutron absorber is the composite containing a concentration of 20% lead because the removal cross-section value is higher than the rest of the values obtained from other concentrations.

When compared to current known shielding materials, this material has the benefit of being able to be applied as a solution to any type of surface, making it more robust for practical applications. This shielding might be used for shielding and transporting radiation materials, as well as for neutron source researches. It also has the benefit of lowering the cost of the radiation shield.

References

[1] G. F. Knoll, *Radiation Detection and Measurement*. New York: John Wiley & Sons Inc., 2010.

[2] S. N. Ahmed, *Physics and Engineering of Radiation Detection.* USA: Academic Press Inc., 2007.

[3] J.K. Shultis and R. E. Faw, *Fundamentals of Nuclear Science and Engineering*. New York: Taylor & Francis Group, 2021.

[4] A. F. Mkhaiber and S. K. Dawood, "Calculation of Shielding Parameters of Fast Neutrons for Some Composite Materials", *Al-Mustansiriyah Journal of Science*, vol. 30, no. 1, pp. 210-215, Aug. 2019.

[5] G. Hu, H. Hu, Q. Yang, B. Yu and W. Sun, "Study on the design and experimental verification of multilayer radiation shield against mixed neutrons and γ-rays", *Nuclear Engineering and Technology*, vol. 52, no. 1, pp. 178–184, Jan. 2020.

[6] S. Thomas, K. Joseph, S. K. Malhotra, K. Goda and M. S. Sreekala, "*Polymer Composites*," Germany: Wiley-VCH Verlag & Co. KGaA, 2012.

[7] InSpector™ 1000 Digital Hand-Held MCA, User's Manual, USA: Canberra Industries, 2003.

[8] A. G. Muslim and A. H. Al-Mashhadani, "Design and Creating a Specific Neutron Irradiation Instrument to Decrease the User's Radiation Exposure Time", *Iraqi Journal of Science*, vol. 64, no. 1, pp. 166–173, Jan. 2023.

[9] N. R. Abd Elwahab, N. Helal, T. Mohamed, F. Shahin and F. M. Ali "New shielding composite paste for mixed fields of fast neutrons and gamma rays," *Materials Chemistry and Physics*, vol. 233, pp. 249-253, 15 May 2019.

[10] J. E. Martin, *Physics for Radiation Protection*. Germany: Wiley-VCH Verlag GmbH & Co. KGaA, 2013.

[11] S.E. Liverhant, *Elementary Introduction to Nuclear Reactor Physics.* New York: John Wiley & Sons, INC., 1960.

[12] Y. Elmahroug, B. Tellili and C. Souga "calculation of fast neutron removal cross-sections for different shielding materials", *International Journal of Physics and Research (IJPR)*, vol. 3, no. 2, pp. 7–16, Jun 2013.

[13] G. Lakshminarayana, I. Kebaili, M. G. Dong, M. S. Al-Buriahi, A. Dahshan, I. V. Kityk, D. Lee, J. Yoon and T. Park, "Estimation of gamma-rays, and fast and the thermal neutrons attenuation characteristics for bismuth tellurite and bismuth boro-tellurite glass systems," *Journal of Materials Science*, vol. 55, no. 14, pp. 5750–5771, May 2020.

[14] A. El-Sayed, "Calculation of the cross-sections for fast neutrons and gamma-rays in concrete shields", *Annals of Nuclear Energy*, vol. 29, no. 16, pp. 1977–1988, Nov. 2002.

[15] B. Alım, E. Şakar, A. Baltakesmez, İ. Han, M. Sayyed and L. Demir, "Experimental investigation of radiation shielding performances of some important AISI-coded stainless steels: Part I", *Radiation Physics and Chemistry*, vol. 166, Jan. 2020.

[16] Z. A. Rahvar, M. Ghorbani, M. Khosroabadi and C. Knaup, "Radiation shielding materials: half-value layer determination for separate and simultaneous photon and neutron emission by a ^{252}Cf source", *International Journal of Radiation Research,* vol. 18, no. 2, pp. 381- 387, Apr. 2020.

[17] A. S. Sameer and A. M. Ali, "Gamma-Ray Shielding Effectiveness of Clay and Boron Doped Clay Material at Different Thicknesses", *Iraqi Journal of Science*, vol. 63, no. 5, pp. 1961–1970, May 2022.